# Separation of blended data by iterative estimation and subtraction of blending interference noise

Araz Mahdad[1], Panagiotis Doulgeris[1], and Gerrit Blacquiere[1]

## ABSTRACT

Seismic acquisition is a trade-off between economy and quality. In conventional acquisition the time intervals between successive records are large enough to avoid interference in time. To obtain an efficient survey, the spatial source sampling is therefore often (too) large. However, in blending, or simultaneous acquisition, temporal overlap between shot records is allowed. This additional degree of freedom in survey design significantly improves the quality or the economics or both. Deblending is the procedure of recovering the data as if they were acquired in the conventional, unblended way. A simple least-squares procedure, however, does not remove the interference due to other sources, or blending noise. Fortunately, the character of this noise is different in different domains, e.g., it is coherent in the common source domain, but incoherent in the common receiver domain. This property is used to obtain a considerable improvement. We propose to estimate the blending noise and subtract it from the blended data. The estimate does not need to be perfect because our procedure is iterative. Starting with the least-squares deblended data, the estimate of the blending noise is obtained via the following steps: sort the data to a domain where the blending noise is incoherent; apply a noise suppression filter; apply a threshold to remove the remaining noise, ending up with (part of) the signal; compute an estimate of the blending noise from this signal. At each iteration, the threshold can be lowered and more of the signal is recovered. Promising results were obtained with a simple implementation of this method for both impulsive and vibratory sources. Undoubtedly, in the future algorithms will be developed for the direct processing of blended data. However, currently a high-quality deblending procedure is an important step allowing the application of contemporary processing flows.

## INTRODUCTION

In current seismic data acquisition, sources are fired with large time intervals in order to avoid interference, leading to time-consuming and expensive surveys. Furthermore, the source side of the acquisition geometry is often coarsely sampled, causing spatial aliasing. The concept of simultaneous acquisition has been introduced to address these issues by either reducing the temporal interval between successive shots, leading to reduced acquisition costs, or by increasing the number of sources within the same survey time, leading to a higher data quality. Note that a combination of the two approaches combines these benefits.

Several authors have discussed the concept of simultaneous and near-simultaneous shooting for impulsive and vibroseis-type sources and their particular advantages. The use of simultaneous vibrators transmitting the same or different reference signals was proposed by Silverman (1979). Beasley et al. (1998) and Beasley (2008) proposed acquiring seismic data by means of simultaneous impulsive sources with large spacing between illuminating shots. The High Fidelity Vibratory Seismic (HFVS) method has been developed by Sallas et al. (1998) in order to increase the productivity of land seismic acquisition and to reduce acquisition costs. Romero et al. (2000) suggested the use of phase encoding in prestack shot record migration such that multiple shots can be migrated simultaneously. Although this work was focused on the migration process, it can be simply generalized to the acquisition phase. Acquiring marine seismic data with random, quasirandom, or systematic delay times between firing sources was proposed by Vaage (2002). Bagaini (2006) discussed various simultaneous vibroseis acquisition methods including simultaneous sweeps, cascaded sweeps, and slip sweeps. The term source blending was introduced by Berkhout (2008), and the differences with plane wave synthesis

(Rietveld and Berkhout, 1994) were pointed out. A near-simultaneous shooting technique with small random time delays between impulsive sources was presented by Hampson et al. (2008). Vibroseis acquisition by means of Simultaneous Pseudorandom Sweep Technology (SPST) has been suggested by Sallas et al. (2008). Berkhout et al. (2009) extended the concept of source blending to the detector side by combining incoherent shooting with incoherent sensing and introducing the concept of double blending.

The separation process (deblending) was addressed as a blind signal separation problem by Ikelle (2007), using independent component analysis as the tool to distinguish between the different blended sources. Lin and Herrmann (2009) and Herrmann et al. (2009), under the umbrella of compressive sensing, use an inversion approach constraining the separated data to be sparse in the curvelet domain. It is worth mentioning that both these approaches use sophisticated source codes (e.g., sweeps or random phase or/and amplitude encoding). Furthermore, Neelamani et al. (2008) have used simultaneous sources and compressive sensing in a similar way to speed up forward modeling.

By reforming the deblending problem into a denoising one, treating the interference due to blending as noise, one can use all kinds of signal processing tools available. It has been reported by various authors — e.g., Moore et al. (2008), Akerberg et al. (2008) — that by sorting the acquired blended data into a different domain than the common source domain (e.g., the common offset domain), the interference noise appears as random spikes; thus, the separation process turns into a typical random noise removal procedure. Based on this property, Huo et al. (2009) use a vector median filter after resorting the data into common mid-point gathers. This 2D filter acts locally and effectively reduces the amplitude of the random spikes. Moore (2010) uses an inversion process with sparsity constraint applied in the radon domain.

Spitz et al. (2008) introduced the idea of building a noise model based on the subsurface's velocity model and the wave equation. The modeled interference noise is adaptively subtracted from the data. Moving a step further, Kim et al. (2009) built a noise model from the data itself and then adaptively sub-

tracted the modeled noise from the acquired data. This algorithm was implemented in the common offset domain and was applied to OBC (ocean bottom cable) data.

In the present work, we developed an iterative noise estimation-and-subtraction process for the effective separation of blended data. A noise model is progressively built from the blended data itself and subsequently subtracted. The method, which can also be formulated as a steepest descent type of method, was applied to field data, where the blending process had been simulated numerically for both impulsive and vibrating sources.

## The concept of source blending and pseudodeblending

Berkhout (1982) showed that seismic data (2D or 3D) can be arranged in the so-called data matrix $\mathbf{P}$. In the temporal frequency domain, each element of $\mathbf{P}$ corresponds to a complex-valued frequency component of a recorded trace, each column represents a shot record, each row represents a detector gather, each diagonal represents a common offset gather, and each anti-diagonal represents a common midpoint gather. Figure 1 illustrates the data matrix. An example of the different gathers extracted from the data matrix is given in Figure 2 for a numerical data set.

A system representation of seismic data is given by the following monochromatic expression (Berkhout, 1982):

$$\mathbf{P}(z_d, z_s) = \mathbf{D}(z_d)\mathbf{X}(z_d, z_s)\mathbf{S}(z_s). \qquad (1)$$

Here $z_s$ and $z_d$ correspond to the source and detector depth level respectively. $\mathbf{S}$ represents the source matrix where each column corresponds to the source wavefield at $z_s$ due to one source (array). $\mathbf{D}$ represents the detector matrix where each row represents one detector (array). The $\mathbf{X}$ matrix is the multidimensional transfer function of the earth, which contains the entire subsurface impulse response, including (internal) multiples, wave conversion, etc. The importance of the source and detector sampling and other acquisition design parameters can be clearly realized from the logical combination of the $\mathbf{D}$ and $\mathbf{S}$ matrices with the $\mathbf{X}$ matrix. If the source and detector side of the acquisition are sparsely sampled or badly designed, $\mathbf{X}$ can not be well represented by $\mathbf{P}$.

The concepts of source blending and incoherent shooting stand for the continuous recording of sources that are encoded with incoherent codes. Source blending is theoretically consistent with plane wave synthesis and controlled source illumination (Rietveld and Berkhout, 1994) in the sense that multiple sources are activated within certain time intervals. However, it differs in the way that the latter methods generate continuous (coherent) wavefronts. In the case of source blending it is important that such wavefronts are not generated. This is because of the spatial band limitation introduced in this way. Instead, we know that the full temporal and spatial bandwidth is preserved in the case that a white, random signal is arriving at every subsurface location, i.e., white within the available bandwidth. By incoherent shooting of the sources in blending we are aiming at preserving the full temporal and spatial bandwidth; see also Lin and Herrmann (2009). In general, source blending can be formulated as follows:

$$\mathbf{P}'(z_d, z_s) = \mathbf{P}(z_d, z_s)\Gamma = \mathbf{D}(z_d)\mathbf{X}(z_d, z_s)\mathbf{S}(z_s)\Gamma, \qquad (2)$$
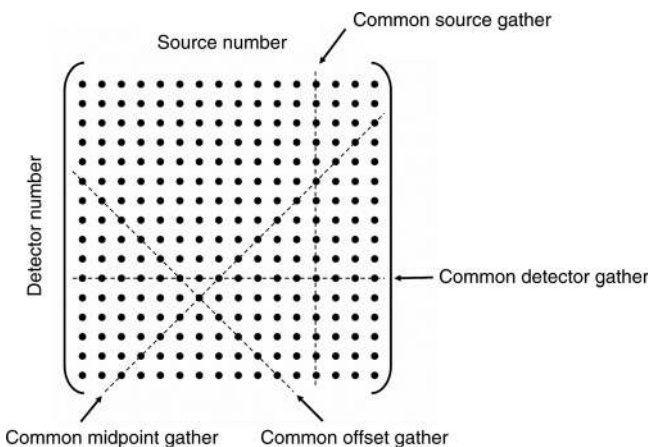


Figure 1. Schematic representation of data matrix. Every element is a complex valued number that represents one frequency component.

where $\mathbf{P}'$ is the blended data matrix. Blending matrix $\Gamma$ contains the blending parameters. Each column $\Gamma_\ell$ is related to a blended shot record and its elements $\Gamma_{k\ell}$ are the source codes that can be phase and/or amplitude terms. For example, in the simple case of a marine survey with random firing times, $\Gamma_{k\ell} = e^{-j\omega\tau_{k\ell}}$ is a linear phase term that expresses the time delay $\tau_{k\ell}$ given to source $k$ in blended source array $\ell$. Similarly, in the case of vibrating sources transmitting a linear sweep, $\Gamma_{k\ell} = e^{-j\beta_{k\ell}\omega^2}$ is a quadratic phase term describing the source code. An example of the different gathers extracted from a blended data matrix and

their $f$-$k$ spectra is given in Figure 3. Here, five shot records from the data set used in Figure 2 were blended. In this example linear phase encoding was applied (corresponding to applying time delays). Note the incoherent structure of the blended data in different domains, and the data compression due to the blending.

To retrieve individual "deblended" shot records from blended data, a matrix inversion has to be performed. In general, the
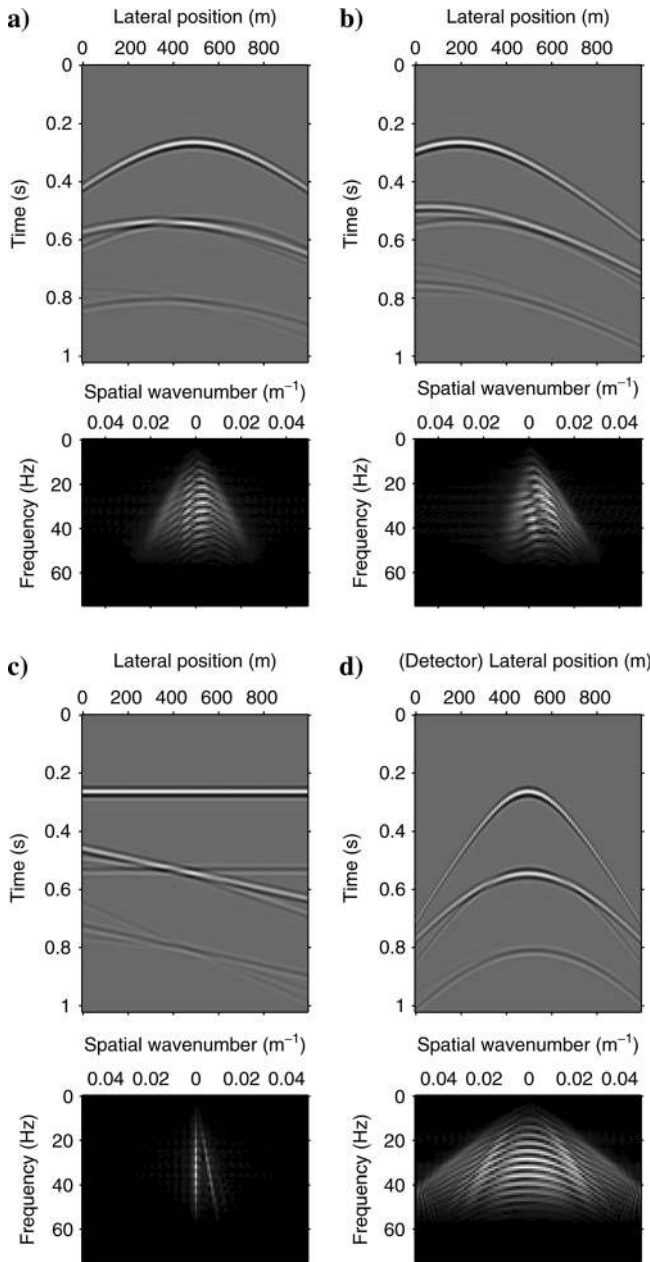


Figure 2. Different sections of the data matrix and their corresponding $f$-$k$ spectra for a numerical data set. (a) One column of the data matrix (common source gather), (b) one row of the data matrix (common detector gather), (c) one diagonal of the data matrix (common offset gather), and (d) one antidiagonal of the data matrix (common midpoint gather).
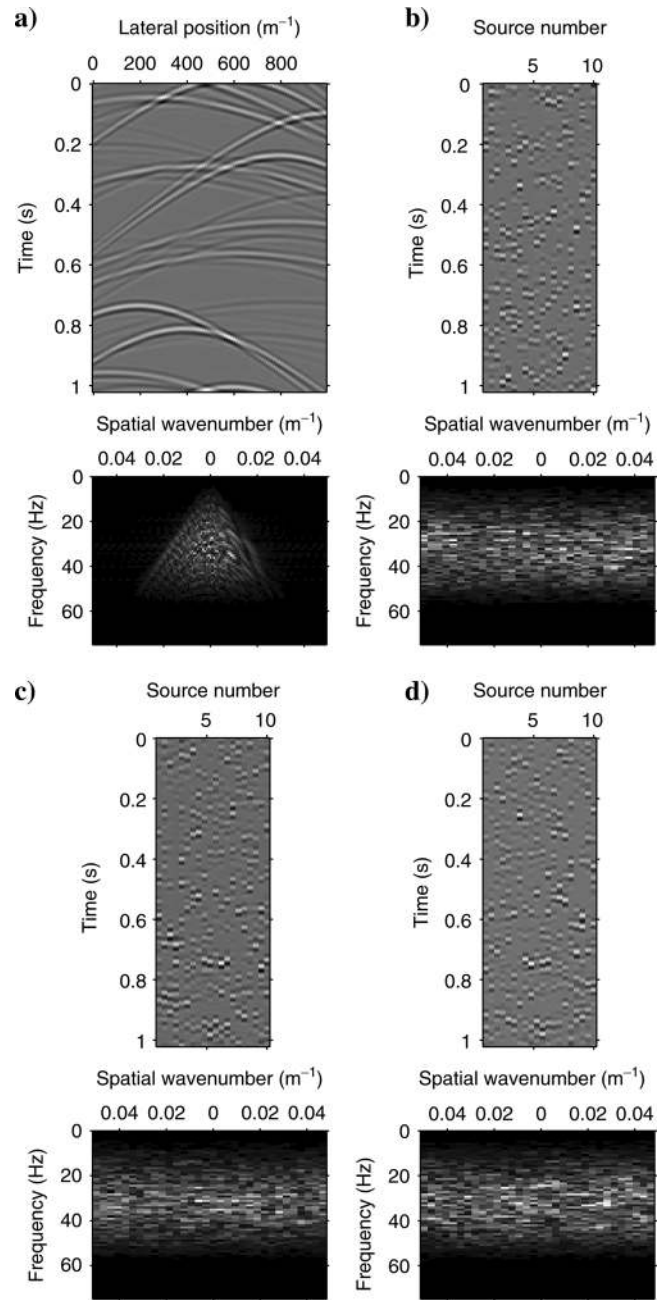
Figure 3. Different sections of the blended data matrix and their corresponding $f$-$k$ spectra for the same data set as shown in Figure 2. The number of sources that are blended together is five. (a) One column of the blended data matrix, (b) one row of the blended data matrix, (c) one diagonal of the blended data matrix, and (d) one antidiagonal of the blended data matrix.

blending problem is underdetermined (i.e., $\mathbf{P}'$ has fewer columns than $\mathbf{P}$), which means that the blending matrix is not invertible. Instead, a least-squares inverse could be used according to

$$\langle \Gamma^{-1}(z_d, z_s) \rangle = \left[ \Gamma^H \Gamma \right]^{-1} \Gamma^H. \tag{3}$$
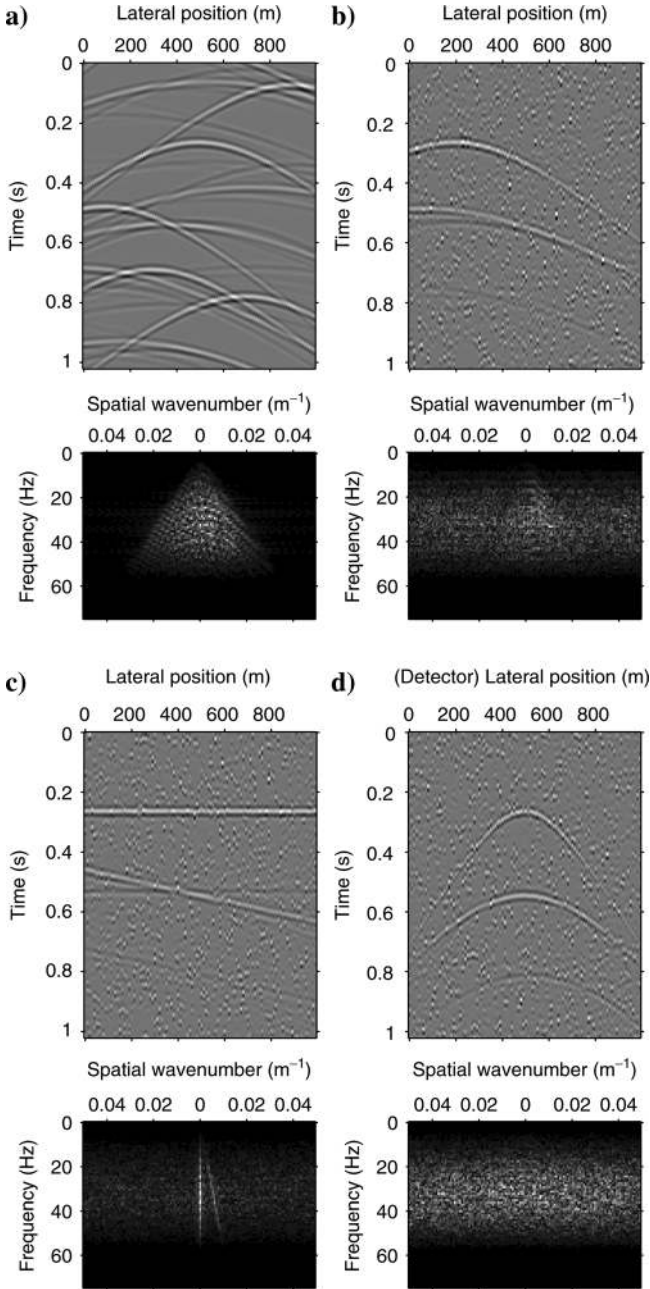
Figure 4. Different sections of pseudodeblended data and their corresponding $f$-$k$ spectra, generated by expanding and restoring the phase applied to the blended data of Figure 3. (a) One column of the pseudodeblended data (common source gather), (b) one row of the pseudodeblended data (common detector gather), (c) one diagonal of the pseudodeblended data (common offset gather), and (d) one antidiagonal of the pseudodeblended data (common midpoint gather).

It can be shown that if the blending matrix only contains phase terms (phase encoding), its least-squares inverse corresponds to the transpose complex conjugate (Hermitian). This leads to the following expression for pseudodeblending:

$$\langle \mathbf{P}(z_d, z_s) \rangle = \mathbf{P}'(z_d, z_s) \Gamma^H. \tag{4}$$

From the physics point of view, the pseudodeblending process carries out an expansion corresponding to the number of sources that are blended together; for example, if this number is $b$, each blended shot record is copied $b$ times. Then, each of these copies is corrected for the corresponding time delays introduced in the field or decoded in the case of encoded sources (correlation). Due to the fact that the responses of multiple sources are included in a single blended shot record and the source codes are not orthogonal, the pseudodeblending process generates correlation noise. This correlation noise is known as "blending noise" or "cross terms." Figure 4 contains an example of different sections of pseudodeblended data recovered from the blended data of Figure 3; the corresponding $f$-$k$ spectra are shown as well. Note the existence of incoherent blending noise in the pseudodeblended common detector and common offset and common midpoint gathers, in contrast with the signal that is coherent in all gathers. The incoherent nature of the blending noise is the discriminating power we will use in the deblending process, to be discussed in detail in the next section.

## METHOD

The blending information contained in $\Gamma$ is known. This means that $\Gamma^H$ is known as well, and therefore, if the unblended data $\mathbf{P}(z_d, z_s)$ were known, the blending noise that is present in the pseudodeblended data $\langle \mathbf{P}(z_d, z_s) \rangle$ could be computed as the difference between the pseudodeblended and the unblended data.

Using equation 4 we obtain

$$\mathbf{N} = \langle \mathbf{P}(z_d, z_s) \rangle - \mathbf{P}(z_d, z_s) = \mathbf{P}'(z_d, z_s) \Gamma^H - \mathbf{P}(z_d, z_s), \tag{5}$$

where $\mathbf{N}$ represents the blending noise. However, the initial unblended data are not available and obviously, if they were, there would be no need for a deblending method. Suppose though, that *part* of $\mathbf{P}(z_d, z_s)$ could be extracted from the pseudodeblended data $\langle \mathbf{P}(z_d, z_s) \rangle$. Then, an iterative estimation-and-subtraction process could be initiated where more of the cross terms could be computed and removed at each iteration. In the following section, we give an intuitive explanation of our iterative method for the separation of blended sources in the common detector domain. The mathematical formulation in the form of a general framework as well as the extension of the method to other domains will be discussed later.

### Iterative deblending in the common detector domain

In the common detector domain, the signal is arranged in coherent events, whereas the cross terms appear as random spikes (see Figures 4b and 5b). Hence, any method that can distinguish between coherent events and random spikes to some degree could be used to suppress the blending interference to some degree (Doulgeris et al., 2010).

A simple example of such a method is a frequency-wavenumber ($f$-$k$) filter that passes only the part of the pseudodeblended data

that resides in the *f-k* band of the signal (i.e., in the signal cone). We propose to compute the signal bandwidth based on the highest velocity observed in the data. The random spikes have a white spectrum in the spatial wavenumber direction, extending out of the signal cone (Figure 4d). Thus, by applying the *f-k* filter, these spikes are somewhat suppressed and we may assume that the highest amplitudes of the pseudodeblended data now belong to the desired signal $\mathbf{P}(z_d, z_s)$ (Figure 5c). Again, any spike removal tool could be used instead of or in combination with the *f-k* filter.

In order to select the unblended part of the data from the output of the filter, we apply a threshold in the *x-t* domain that keeps only the parts of the signal that have an amplitude higher than a certain predefined value (e.g., 0.9 times the maximum amplitude present). Note that alternatively the application of the threshold could take place in the filtering domain (in this example, *f-k*), being integrated in this way in the filtering process. This thresholding process is shown in Figure 5d. Note that, ideally, after the thresholding process no blending noise is present anymore. In practice, there may be some leakage of blending noise. The consequence of this will be discussed later.

We can now predict part of the blending noise, based on the output of the previous step. This output contains part of the unblended data, so by applying the blending matrix $\Gamma$ to it we can simulate the blending that took place in the field. Then, we can apply the pseudodeblending process via $\Gamma^H$, producing in this way data that contain part of the unblended data as well as the cross terms that were created by that part. Because that part of the unblended data is known, it can be subtracted, resulting in only the cross terms. Using the matrix formulation, this could be summarized as multiplying the known part of the unblended data by a term $(\Gamma\Gamma^H - \mathbf{I})$. Hence, an estimate of the blending noise has now been computed (Figure 5e).

At this point, we can subtract this blending-noise estimate from the pseudodeblended data. In the case that the blending parameters are not known exactly, the subtraction could be carried out in an adaptive way. The new estimate of the unblended data, which has less blending noise, can now serve as the updated input to the *f-k* filter (or in fact any spike removal filter). The filter output is expected to contain less blending noise than in the previous iteration, so that the threshold can be lowered, leading to an even better estimate of the blending noise.

Repeating this process leads to the gradual removal of cross terms from the pseudodeblended gather, until no further improvement is achieved. A criterion has been implemented to monitor and terminate the iterative procedure (see the next section). Once terminated, the last output of the filter is taken as the deblended common detector gather (Figure 5f). Figure 5g displays a shot record of the final deblended data.

As mentioned, after thresholding some blending noise may still be present. For example, think of a weak cross term interfering with a strong signal event such that it partly passes the threshold. In our experience, this type of leaked blending noise appears to spread out spatially and decrease its amplitude in the course of the highly nonlinear iterative process. Note, that a better incoherency filter might do a much better job than our simple thresholding procedure. Still, it is our belief that this leakage sets a lower bound on the residual blending noise in the final result. However, this is a subject of further research.

As a final remark we mention that a common detector gather has a unique property that can prove very useful in the imple-

mentation of the algorithm. Namely, the blending noise present in the gather after pseudodeblending is solely produced by the signal present in the very same gather. This stems from the fact that all the sources are present in each common detector gather. It follows that each pseudodeblended common detector gather can be treated individually. This means that the algorithm can be very easily parallelized when implemented in the common detector domain.

## Convergence and stopping criterion

The algorithm iterates to the correct solution if no blending noise remains in the output of the thresholding process and, for convergence, the threshold decreases at each iteration. These requirements rely on the sequence of thresholds chosen during the execution of the algorithm. We can predefine the thresholds or set them during execution. As a rule of thumb, a predefined sequence of the form $n^i$, where $i$ is the iteration number and $n$, being the threshold at the first iteration, is chosen as $n \geq 0.9 \times \max\{\mathbf{P}'(z_d, z_s)\}$, is a safe choice. On the other hand, setting the threshold manually after inspection of the results at each iteration gives an extra degree of freedom that can be used to fine-tune the process and leads to faster convergence.

The stopping criterion is based on an energy measure that is computed as follows. The deblended output of each iteration is
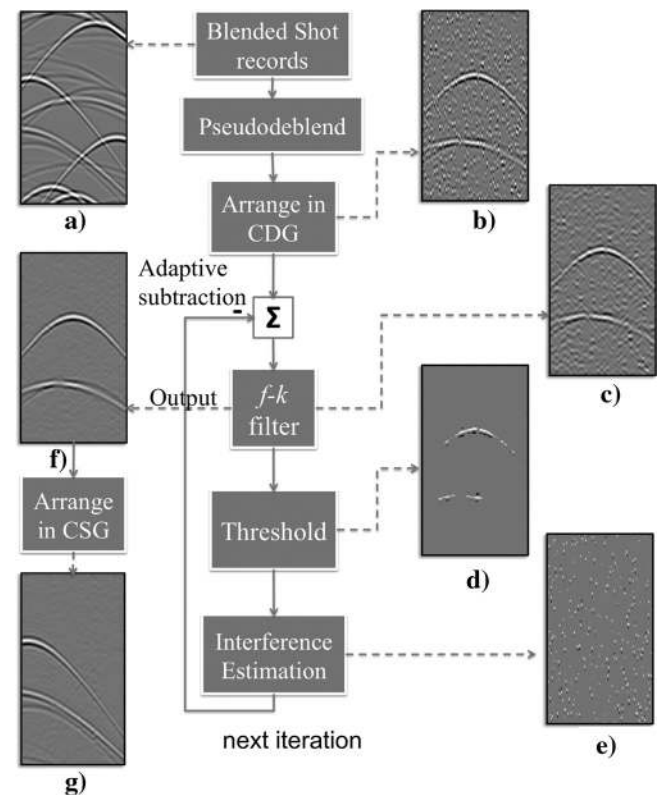


Figure 5. The flow chart of the deblending algorithm (CDG, common detector gather; CSG, common source gather). (a) Blended common source gather, (b) pseudodeblended common detector gather, (c) the output of the *f-k* filter on the first iteration, (d) the output of the thresholding process on the first iteration, (e) the blending-noise estimate on the first iteration, (f) the deblended common detector gather, and (g) the deblended common source gather.

blended again by applying the blending matrix $\Gamma$ and is then subtracted from the corresponding blended shot record as it was acquired in the field; the root mean square of this difference, once integrated over the record, provides the measure. The iterative procedure is stopped once this measure is no longer decreasing or when it is lower than a predefined value.

## Iterative deblending in other domains

The iterative deblending method can also be implemented in domains other than the common detector domain, for example, in the common offset, common midpoint, or common source domain. Some of the properties of the algorithm will now be discussed for each of these domains.

### Common offset domain

The noise removal filter involved in our method requires a sufficiently large number of traces in each gather to be processed. In many acquisition configurations, the common offset domain offers the largest gathers, making it a good choice for this method.

Another interesting property of the pseudodeblended common offset gathers is displayed in Figure 6. The signal-to-blending noise ratio varies among different common offset gathers. Near-offset gathers tend to contain high-amplitude signal and lower-amplitude interference (Figure 6a). On the other hand, far-offsets tend to have lower-amplitudes, thereby suffering more from the blending noise from all the other offsets (in particular from the strong near-offsets; see Figure 6c). Treating the different bands of offsets sequentially and starting with the near-offsets allows the method to process data with more blending noise faster. By the time the algorithm starts processing the far-off-

sets, most of the cross terms that were caused by the near- and mid-offsets will have been removed. Information on the particular blended acquisition geometry used here is given in the subsection "Application to impulsive sources."

### Common midpoint domain

Our method can also be implemented in the common midpoint (CMP) domain. Applying normal moveout correction to a pseudodeblended common midpoint gather forces the signals' $f$-$k$ spectrum to be concentrated in a narrow-band cone. On the other hand, the cross terms still have a white spectrum in the spatial wavenumber direction. Hence, an $f$-$k$ filter can suppress the cross terms better in the CMP domain than in other domains.

### Common source domain

Because the cross terms have a coherent structure in the common source domain (see Figure 4b), a spatial filter (e.g., an $f$-$k$ filter) is not able to discriminate the desired signal from the cross terms. However, the use of sophisticated source codes, such as incoherent sweeps or random phase, may result in cross terms with a lower amplitude level than that of the signal. Therefore, thresholding can be done directly after pseudodeblending without the need for a spatial filter. However, depending on the cross-term structure, different types of filters could be applied prior to thresholding (e.g., time-frequency filters) to suppress the cross-term energy further. An advantage of the common source domain is that the deblending process can be executed per blended shot record, which may result in an efficient implementation.

## General framework

The iterative deblending method can be generalized to work on the data matrix $\mathbf{P}(z_d, z_s)$ as a whole rather than on subsets such as common detector gathers individually. Dropping the depth variables $z_d$ and $z_s$ as well as the brackets from the deblended estimate for notational convenience, the general framework can be formulated as

$$\mathbf{P}^{i+1} = \mathbf{P}'\Gamma^H - \overline{\mathbf{P}^i}\left(\Gamma\Gamma^H - \mathbf{I}\right), \tag{6}$$

where $\mathbf{P}^{i+1}$ is the deblended estimate at iteration $i+1$ and $\overline{\mathbf{P}^i}$ is the deblended estimate at iteration $i$ processed in such a way that only (part of) the signal is contained. The $f$-$k$ filtering and thresholding, as described earlier, is a simple example of such a processing step. However, the domain-specific filter can now be replaced by a multidimensional filter. Such a filter can take even better advantage of the lateral consistency of the seismic data versus the incoherency of the blending noise. In fact, any (multidimensional) denoising technology can be integrated into this step.

The second term on the right-hand side of equation 6 transforms the estimated unblended data $\overline{\mathbf{P}^i}$ into blending noise. This is achieved by applying both blending and pseudodeblending via multiplication with $\Gamma\Gamma^H$, while making sure that the initial signal is removed by subtracting $\overline{\mathbf{P}^i}\mathbf{I}$.

It is interesting to notice that an alternative way of deriving equation 6 can be obtained by formulating deblending as an optimization problem and solving it with a steepest-descent type method. The optimization problem could be written as
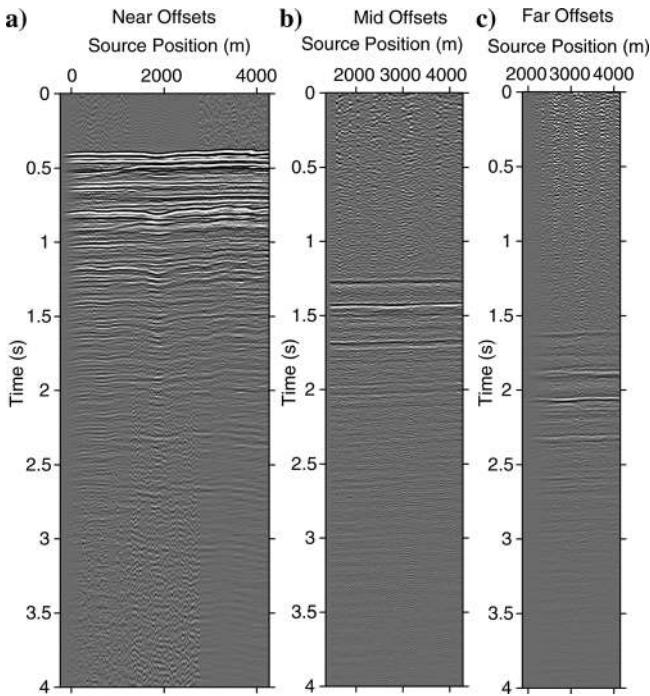


Figure 6. Pseudodeblended common offset gathers. (a) Near-offset gather, (b) mid-offset gather, and (c) far-offset gather.

$$\text{minimize } f(\mathbf{P}) = \frac{1}{2}\|\mathbf{P}' - \mathbf{P}\Gamma\|_2^2 \qquad (7)$$

$$\text{subject to}|C_{\mathbf{P}}| > \beta,$$

where $C_{\mathbf{P}}$ denotes a normalized coherency measure of the data, (e.g., normalized crosscorrelation or semblance coefficient, integrated over the whole dataset; see Neidell and Taner, 1971). The absolute value of this coherency measure takes values in the interval 0,1 with values close to 1 showing high coherency. It follows that the parameter $\beta$ takes values in the same interval.

Ignoring, for the moment, the inequality constraint in Equation 7, a steepest descent iteration in matrix notation would be

$$\mathbf{P}^{i+1} = \mathbf{P}^i + \alpha^{i+1}\left(\mathbf{P}' - \mathbf{P}^i\Gamma\right)\Gamma^H, \qquad (8)$$

with $\mathbf{P}^0 = 0$ and $\alpha$ being the step length. In the absence of noise in the forward model, i.e., when the blending parameters are known precisely, the blending matrix $\Gamma$ can be chosen such that the diagonal of the $\Gamma\Gamma^H$ matrix is populated with ones. In this case, the parameter $\alpha$ should be equal to 1. Equation 8 can then be written as

$$\mathbf{P}^{i+1} = \mathbf{P}'\Gamma^H - \mathbf{P}^i\left(\Gamma\Gamma^H - \mathbf{I}\right). \qquad (9)$$

In order to take into account the inequality constraint in Equation 6, a projection of the current estimate onto the feasible set is required, i.e., the set of coherent signals in the model space. This projection can be implemented as a coherency-pass filter. If we denote the projected $\mathbf{P}^i$ as $\overline{\mathbf{P}^i}$, then Equation 6 is obtained. Note that this means that our method belongs to the class of inversion type of methods. Other examples of such methods are Abma and Yan (2009) and Abma et al. (2010).

## RESULTS

We now demonstrate how this approach performs when applied to marine field data with two examples, one for encoded sources and one for impulsive sources. We applied numerical blending to a data set that was acquired using a traditional acquisition design by Statoil in the Haltenbanken field, in Norway. The temporal and spatial sampling interval for this example are 4 ms and 25 m, respectively.

### Application to encoded sources

As stated before, the deblending process can be performed in the common source domain as long as the sources are encoded with sophisticated incoherent codes. The process of deblending has been carried out for a blended record containing two marine shot records. Each shot record contains 281 traces and 1024 time samples. In this example, the shot records, which were acquired with an air-gun source, are encoded with up-sweep and down-sweep signals of 6 seconds, respectively, and blended numerically. The result can be interpreted as the recording of two marine vibrators firing simultaneously with mentioned sweeps. The two original shot records and the blended shot record are shown in Figure 7. The deblending results, obtained after 67 iterations, are depicted in Figure 8, and can be compared with the pseudodeblended results.
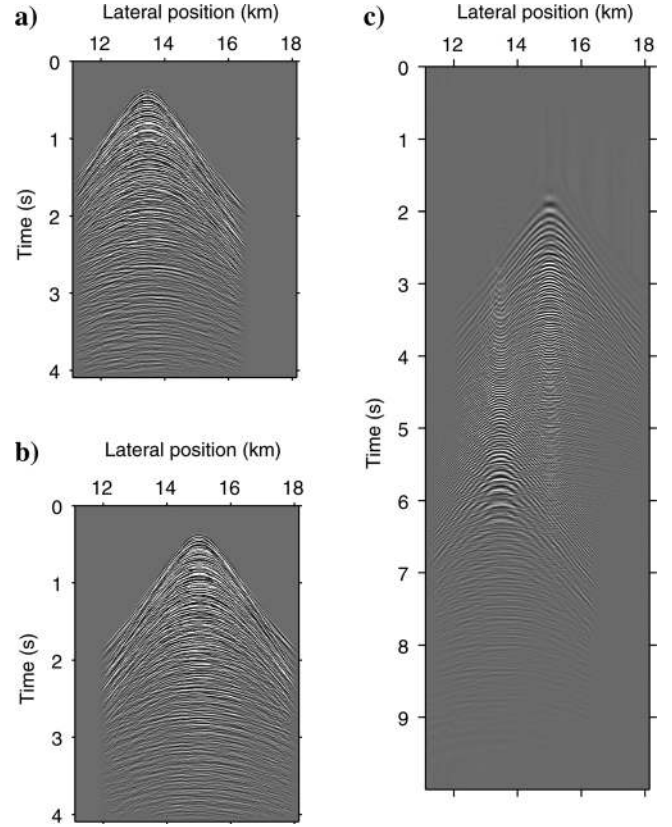


Figure 7. (a) Marine shot record 1, (b) marine shot record 2, and (c) numerically blended shot record (sum of two encoded shot records).
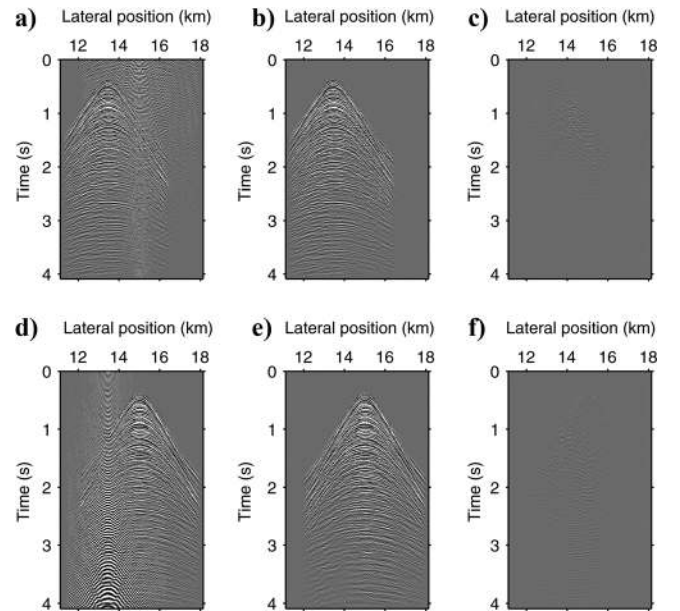


Figure 8. (a) Pseudodeblended shot record 1, (b) deblended shot record, (c) difference of deblended and unblended shot record 1 (8b–7a), (d) pseudodeblended shot record 2, (e) deblended shot record 2, and (f) difference of deblended and unblended shot record 2 (8c–7b).

Note the cross terms that are still present in the pseudodeblended results. Records containing the residual cross-term energy are also shown. As illustrated, the two shot records have been deblended almost perfectly. The signal-to-blending noise ratio (S/N) after $n$ iterations is calculated as follows:

$$S/N = 20 \log_{10} \frac{\mathbf{P}_{rms}}{(\mathbf{P}^n - \mathbf{P})_{rms}}, \qquad (10)$$

where the subscript rms stands for root mean square; the mean being computed over all elements of $\mathbf{P}$ as well as overall frequency components. The S/N of the deblended shot records is 27 dB. In practice, equation 10 cannot be used because the unblended data are not available. However, this S/N definition provides the most direct measure of separability and could be computed in our examples because blending was performed numerically.

Note that in practice the use of downsweeps is often avoided because of the presence of harmonics (Abd El-Aal, 2010). Alternatives are the use of upsweeps with different lengths or, in the case of the same sweep length for all sources, application of the method in one of the other domains discussed earlier.

## Application to impulsive sources

We have simulated a 2D blended marine survey based on a subset of the unblended data set of the previous example. The blended acquisition design consists of one streamer in which three sources fire with small random time delays. The detectors of the streamer record the responses of all three sources, resulting in blended shot records that contain negative offsets as well as very small offsets. We obtained the negative-offset traces via reciprocity. In addition, the missing near-offsets were obtained via interpolation. Note that the offset range is not the same for the three sources because of this special acquisition configuration. Figure 9a shows a shot record after the aforementioned processing. The same shot record after pseudodeblending can be seen in Figure 9b. Notice that the three different shot records that were involved in the blending process can still be recognized. The S/N of this shot record — as far as blending noise is concerned — is around −6 dB, i.e., more noise than signal.

The deblending procedure was carried out in the common offset domain. The near-offsets were processed first until no further improvement could be achieved; the mid- and far-offsets followed. The filter used for this example is a simple $f$-$k$ filter and the thresholding process takes place in the $x$-$t$ domain. Figure 9c shows the deblended estimate obtained after 26 iterations. So far only the near-offsets have been used to estimate and subtract the blending noise. Figure 9d shows the results after 36 iterations where the algorithm had finished processing the mid-offsets. The final result, obtained after 44 iterations when processing the far-offsets was finished and no further improvement could be achieved, is shown in Figure 9e. Although some residual energy is left (see Figure 9f), the result is close to the desired output, with the S/N being approximately 12 dB. Hence, the enhancement, in terms of S/N, achieved by the simple implementation of the algorithm in this example is around 18 dB.

## DISCUSSION

In this paper we introduced a general framework for the separation of blended data. The result is a data set as if it were acquired without blending. The major benefit of the method is that the data can be processed further with the current, existing algorithms and available tools. However, we realize that in the future the processing of blended data will most likely be direct, i.e., with new algorithms that are capable of handling blended data without the need for a deblending step, e.g., see Verschuur and Berkhout (2010). In this context, this method can be regarded as a necessary transition step toward this direction. Furthermore, we envision that even in the case of direct processing of blending data, a deblending algorithm may still be applicable as a valuable tool at the preprocessing stage.
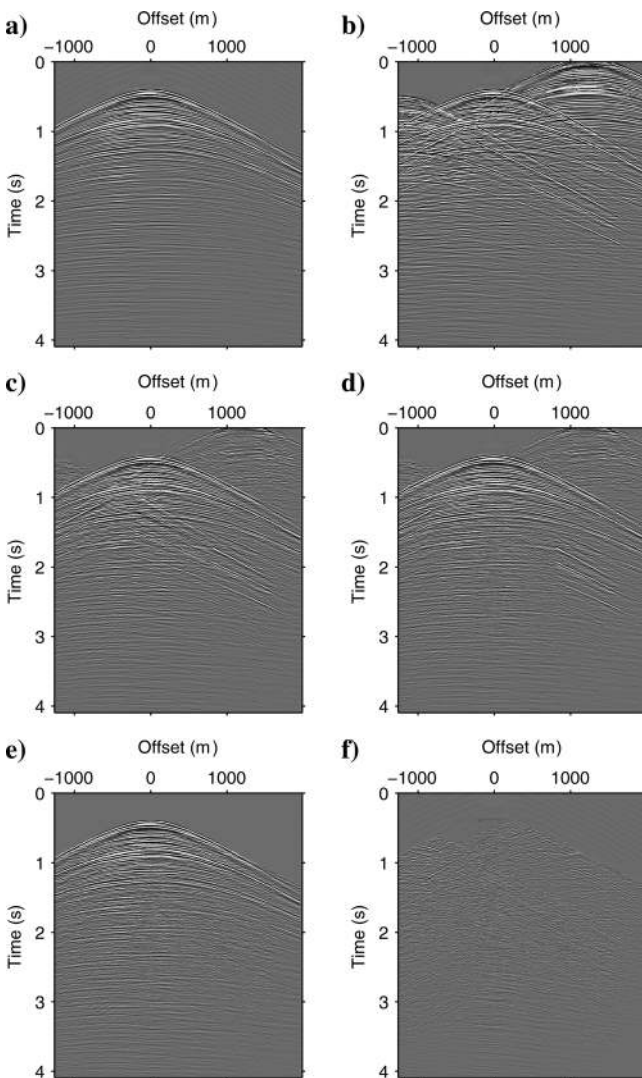


Figure 9. (a) Unblended shot record, (b) initial estimate (pseudodeblended result), (c) estimate after 26 iterations, (d) estimate after 36 iterations, (e) final deblended result after 44 iterations, and (f) residual energy.

## CONCLUSIONS

The emerging concept of blended or simultaneous sources promises higher quality seismic data at lower cost. Although the direct processing of blended data may prove to be the way to go, separation algorithms can facilitate the transition from traditional to blended techniques by providing a way to process blended data with contemporary processing tools. In this paper, we have introduced a framework for the separation of blended data based on the iterative estimation and subtraction of blending noise. In an optimization context, this could be expressed as a steepest-descent type of method for solving regularized least-squares problems.

This method can be implemented in the common source, common detector, common offset, or common midpoint domain, benefiting from the special properties of blended data in each of these. Typically, the nature of the survey should dictate the most suitable domain. Furthermore, this method can handle both vibrating and impulsive sources and can integrate any existing denoising technique for the extraction of unblended data from the pseudodeblended data. The method can be generalized to integrate the various domains in such a way that the domain-specific advantages are combined.

We have applied a simple implementation of this iterative scheme to field data that were blended numerically, using impulsive as well as vibrating sources, producing promising results.

## ACKNOWLEDGMENTS

## REFERENCES

Abd El-Aal, 2010, A. K. Eliminating upper harmonic noise in vibroseis data via numerical simulation: Geophysical Journal International **181**, 1499–1509 (2010).

Abma, R. T. Manning, M. Tanis, J. Yu, and M. Foster, 2010, High quality separation of simultaneous sources by sparse inversion: 72nd Annual International Meeting, EAGE, Extended Abstracts, B003.

Abma, R., and J. Yan, 2009, Separating simultaneous sources by inversion: 71st Annual International Meeting, EAGE, Expanded Abstracts, V002.

Akerberg, P. G. Hampson, H. Richett, H. Martin, and J. Cole, 2008, Simultaneous source separation by sparse radon transform: 78th Annual International Meeting, SEG, Expanded Abstracts, 2801–2804.

Bagaini, C., 2006, Overview of simultaneous vibroseis acquisition methods: 76th Annual International Meeting, SEG, Expanded Abstracts, 70–74.

Beasley, C. J., 2008, A new look at marine simultaneous sources: The Leading Edge, **27**, no. 7, 914–917, doi:10.1190/1.2954033.

Beasley, C. J. R. E. Chambers, and Z. Jiang, 1998, A new look at simultaneous sources: 68th Annual International Meeting, SEG, Expanded Abstracts, 133–135.

Berkhout, A. J., 1982, Seismic migration, imaging of acoustic energy by wave field extrapolation, A. Theoretical aspects: Elsevier.

Berkhout, A. J. G., 2008, Changing the mindset in seismic data acquisition: The Leading Edge, **27**, no.7, 924–938, doi:10.1190/1.2954035.

Berkhout, A. J. G. Blacquière, and D. J. Verschuur, 2009, The concept of double blending: Combining incoherent shooting with incoherent sensing: Geophysics, **74**, no.4, A59–A62, doi:10.1190/1.3141895.

Doulgeris, P. A. Mahdad, and G. Blacquière, 2010, Separation of blended impulsive sources using an iterative approach: 72nd Annual International Meeting, EAGE, Extended Abstracts, B004.

Hampson, G. J. Stefani, and F. Herkenhoff, 2008, Acquisition using simultaneous sources: The Leading Edge, **27**, no.7, 918–923, doi:10.1190/1.2954034.

Herrmann, F. Y. Erlangga, and T. Lin, 2009, Compressive simultaneous full-waveform simulation: Geophysics, **74**, no.4, A35–A40, doi:10.1190/1.3115122.

Huo, S. Y. Luo, and P. Kelamis, 2009, Simultaneous sources separation via multi-directional vector-median filter: 79th Annual International Meeting, SEG, Expanded Abstracts, 31–35.

Ikelle, L., 2007, Coding and decoding: Seismic data modeling, acquisition and processing: 77th Annual International Meeting, SEG, Expanded Abstracts, 66–70.

Kim, Y. I. Gruzinov, M. Guo, and S. Sen, 2009, Source separation of simultaneous source obc data: 79th Annual International Meeting, SEG, Expanded Abstracts, 51–55.

Lin, T. T. Y., and F. J. Herrmann, 2009, Designing simultaneous acquisitions with compressive sensing: 71st Annual International Meeting, EAGE, Extended Abstracts, S006.

Moore, I., 2010, Simultaneous sources — processing and applications: 72nd Annual International Meeting, EAGE, Extended Abstracts, B001.

Moore, I. W. Dragoset, T. Ommundsen, D. Wilson, C. Ward, and D. Eke, 2008, Simultaneous source separation using dithered sources: 78th Annual International Meeting, SEG, Expanded Abstracts, 2806–2809.

Neelamani, N. C. Krohn, J. Krebs, M. Deffenbaugh, and J. Romberg, 2008, Efficient seismic forward modeling using simultaneous random sources and sparsity: 78th Annual International Meeting, SEG, Expanded Abstracts, 2107–2111.

Neidell, N. S., and M. T. Taner, 1971, Semblance and other coherency measures for multichannel data: Geophysics, **36**, 482–497, doi:10.1190/1.1440186.

Rietveld, W., and A. Berkhout, 1994, Prestack depth migration by means of controlled illumination: Geophysics, **59**, 801–809, doi:10.1190/1.1443638.

Romero, L. A. D. C. Ghiglia, C. C. Ober, and S. A. Morton, 2000, Phase encoding of shot records in prestack migration: Geophysics, **65**, 426–436, doi:10.1190/1.1444737.

Sallas, J., D. Corrigan, and K. P. Allen, 1998, High-fidelity vibratory source method with source separation: U.S. patent **5** 721, 710.

Sallas, J. J. Gibson, F. Lin, O. Winter, B. Montgomery, and N. P., 2008, Broadband vibroseis using simultaneous pseudorandom sweeps: 78th Annual International Meeting, SEG, Expanded Abstracts, 100–104.

Silverman, D., 1979, Method of three dimensional seismic prospecting: U.S.Patent **4**, 159, 463.

Spitz, S. G. Hampson, and A. Pica, 2008, Simultaneous source separation: A prediction subtraction approach: 78th Annual International Meeting, SEG, Expanded Abstracts, 2811–2814.

Vaage, S., 2002, Method and system for acquiring marine seismic data using multiple sources: U.S. Patent **6**, 906, 981 B2.

Verschuur, D. J., and A. J. Berkhout, 2010, Angle-dependent least-squares imaging of incoherent wavefields: 72nd Annual International Meeting, EAGE, Extended Abstracts, C010.